# DFT and TD-DFT Calculations of Some Metal Free Phthalonitrile Derivatives for Enhancement of the Dye Sensitized Solar Cells

P.M. Anbarasan[a,*], P. Senthil Kumar[a], K. Vasudevan[a], S. Moorthy Babu[b] and V. Aroulmoji[c]

[a]Department of Physics, Periyar University, Salem — 636 011, India

[b]Crystal Growth Centre, Anna University, Chennai — 600 025, India

[c]PROTOS Research Institute, Via Flavia 23/1, C/O Sviluppo Italia, 34147 Trieste, Italy

*(Received January 1, 2010; revised version April 20, 2010; in final form May 10, 2010)*

The geometries, electronic structures, polarizabilities, and hyperpolarizabilities of organic dye sensitizers 3,4-pyridinedicarbonitrile, 3-aminophthalonitrile, 4-aminophthalonitrile and 4-methylphthalonitrile were studied based on density functional theory using the hybrid functional B3LYP. Ultraviolet-visible spectra were investigated by time dependent density functional theory. The features of electronic absorption spectra in the visible and near-UV regions were assigned based on time dependent density functional theory calculations. The absorption bands are assigned to $\pi \rightarrow \pi^*$ transitions. Calculated results suggest that the three lowest energy excited states of 3,4-pyridinedicarbonitrile, 3-aminophthalonitrile, 4-aminophthalonitrile and 4-methylphthalonitrile are due to photoinduced electron transfer processes. The interfacial electron transfer between semiconductor $TiO_2$ electrode and dye sensitizers 3,4-pyridinedicarbonitrile, 3-aminophthalonitrile, 4-aminophthalonitrile and 4-methylphthalonitrile is due to an electron injection process from excited dyes to the semiconductor's conduction band. The role of amide and methyl groups in phthalonitrile in geometries, electronic structures, and spectral properties were analyzed in a comparative study of 3,4-pyridinedicarbonitrile, 3-aminophthalonitrile, 4-aminophthalonitrile and 4-methylphthalonitrile for the improvement of dye sensitized solar cells.

PACS: 78.66.Qn, 31.10.+z, 71.15.Mb, 32.30.−r

## 1. Introduction

New technologies for direct solar energy conversion have gained more attention in the last few years. In particular, dye sensitized solar cells (DSSCs) are promising in terms of efficiency and low cost [1–3]. The leading feature of DSSC consists in a wide band gap nanocrystalline film grafted with a quasi-monolayer of dye molecules and submerged in a redox electrolyte. This elegant architecture can synchronously address two critical issues of employing organic materials for the photovoltaic applications: (i) efficient charge generation from the Frenkel excitons and (ii) long-lived electron–hole separation up to the millisecond time domain. The latter attribute can often confer an almost quantitative charge collection for several micrometer-thick active layers, even if the electron mobilities in nanostructured semiconducting films are significantly lower than those in the bulk crystalline materials. Benefited from systematic device engineering and continuous material innovation, a state of the art DSSC with a ruthenium sensitizer has achieved a validated efficiency of 11.1% [4] measured under the Air Mass 1.5 Global (AM1.5G) conditions. In view of the limited ruthenium resource and the heavy-metal toxicity, metal-free organic dyes have received surging research interest in recent years [5–21]. Because of their high molar absorption coefficient, relatively simple synthesis procedure, various structures and lower cost in contrast to a ruthenium dye and the flexibility in molecular tailoring of an organic sensitizer provides a large area to explore [22–24]. In addition, recently a rapid progress of organic dyes has been witnessed reaching close to 10.0% efficiencies in combination with a volatile acetonitrile-based electrolyte [25]. In this paper the performance of following metal free dyes that can be used in DSSC namely 3,4--pyridinedicarbonitrile, 3-aminophthalonitrile, 4-aminophthalonitrile and 4-methylphthalonitrile is analyzed.

## 2. Computational methods

The computations of the geometries, electronic structures, polarizabilities and hyperpolarizabilities for dye sensitizers 3,4-pyridinedicarbonitrile, 3-aminophthalonitrile, 4-aminophthalonitrile and 4-methylphthalonitrile were done using density functional theory (DFT) with Gaussian 03 package [26]. The DFT was treated with hybrid functional Becke's three parameter gradient--corrected exchange potential and the Lee–Yang–Parr (B3LYP) [27–29]. The calculations were performed without any symmetry constraints by using polarized triple--zeta 6-311++G(d,p) basis sets. The vibrational wave numbers were also calculated with the same method and the calculated Raman activities ($S_i$) were converted to relative Raman intensities ($I_i$) using the following relationship derived from the intensity theory of the Raman scattering [30–32]:

* corresponding author; e-mail: anbarasanpm@gmail.com

$$I_i = \frac{f\left(\nu_0 - \nu_i\right)^4 S_i}{\nu_i\left[1 - \exp(hc\nu_i/kt)\right]},$$

where $\nu_0$ is the exciting wave number in $\mathrm{cm}^{-1}$, $\nu_i$ is the vibrational wave number of the $i$-th normal mode, $h$, $c$ and $k$ are fundamental constants and $f$ is a suitably chosen common normalization factor for all peak intensities. Simulation of calculated IR and Raman spectra have been plotted using pure Lorentzian band shape with a bandwidth (FWHM) of 10 $\mathrm{cm}^{-1}$. The electronic absorption spectra require calculation of the allowed excitations and oscillator strengths. These calculations were done using TD-DFT with PBE1PBE [20] correlation functional and same 6-311++G(d,p) basis sets in vacuum and solution, and the non-equilibrium version of the polarizable continuum model (PCM) [33, 34] was adopted for calculating the solvent effects.

## 3. Results and discussion

### 3.1. The geometric structures

The optimized geometries of the 3,4-pyridinedicarbonitrile, 3-aminophthalonitrile, 4-aminophthalonitrile and 4-methylphthalonitrile are shown in Fig. 1, and the selected bond lengths, bond angles and dihedral angles are listed in Table I. The similar geometrical character induces the similar geometrical parameters of 3,4--pyridinedicarbonitrile, 3-aminophthalonitrile, 4-aminophthalonitrile and 4-methylphthalonitrile. Among these dyes 4-aminophthalonitrile has the largest conjugate bridge between carbonyl and amide group.

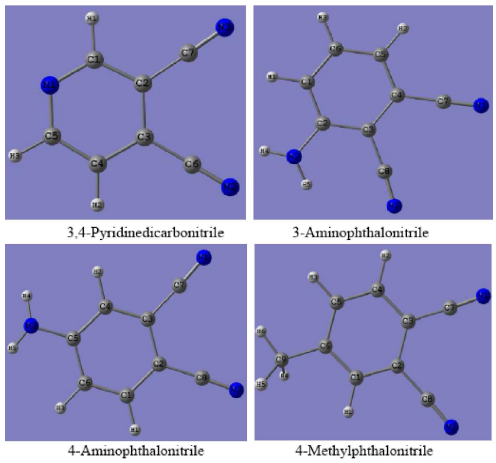


Fig. 1. Optimized geometrical structures of dyes 3,4--pyridinedicarbonitrile, 3-aminophthalonitrile, 4-aminophthalonitrile, and 4-methylphthalonitrile with atomic serial numbers.

TABLE I

Selected bond lengths (in Å), bond angles (in degree) and dihedral (in degree) of the dyes 3,4-pyridinedicarbonitrile, 3-aminophthalonitrile, 4-aminophthalonitrile, and 4-methylphthalonitrile.

| 3,4-pyridinedicarbonitrile | | 3-aminophthalonitrile | | 4-aminophthalonitrile | | 4-methylphthalonitrile | |
|---|---|---|---|---|---|---|---|
| C2–C3 | 1.4095 | C2–C3 | 1.4169 | C2–C3 | 1.4131 | C2–C3 | 1.4131 |
| C2–C7 | 1.4269 | C2–N3 | 1.3691 | C2–C8 | 1.4255 | C2–C8 | 1.4306 |
| C3–C6 | 1.4299 | C3–C4 | 1.4144 | C3–C7 | 1.4314 | C3–C7 | 1.4291 |
| C6–N2 | 1.154 | C3–C8 | 1.4232 | C5–N3 | 1.3774 | C6–C9 | 1.5073 |
| C7–N3 | 1.1545 | C4–C7 | 1.4307 | C7–N1 | 1.1548 | C7–N1 | 1.1551 |
| C1–C2–C7 | 119.843 | C2–C1–H1 | 118.9322 | C2–C1–H1 | 118.9278 | C2–C1–C6 | 121.3942 |
| C3–C2–C7 | 122.1911 | C6–C1–H1 | 120.0877 | C6–C1–H1 | 119.8277 | C2–C1–H1 | 118.5861 |
| C2–C3–C4 | 118.2039 | C1–C2–C3 | 118.1636 | C1–C2–C3 | 118.241 | C6–C1–H1 | 120.0196 |
| C2–C3–C6 | 121.5964 | C1–C2–N3 | 120.9201 | C1–C2–C8 | 119.9354 | C1–C2–C3 | 119.725 |
| C4–C3–C6 | 120.1997 | C3–C2–N3 | 120.8926 | C3–C2–C8 | 121.8236 | C1–C2–C8 | 119.1516 |
| C3–C4–C5 | 118.7099 | C2–C3–C4 | 120.054 | C2–C3–C4 | 120.4646 | C3–C2–C8 | 121.1233 |
| C1–N1–C5 | 117.8072 | C4–C5–C6 | 119.0469 | C4–C5–C6 | 118.4398 | C5–C4–H2 | 120.3986 |
| N1–C1–C2–C3 | 0.0018 | C6–C1–C2–N3 | 178.0814 | C6–C1–C2–C3 | 0.015 | C6–C1–C2–C8 | 180.0004 |
| N1–C1–C2–C7 | 180.0012 | H1–C1–C6–C5 | 179.6242 | H1–C1–C2–C3 | 179.953 | H1–C1–C2–C8 | 0.0006 |
| H1–C1–N1–C5 | 180.0022 | C1–C2–C3–C4 | 0.2714 | H1–C1–C2–C8 | 0.0431 | C2–C1–C6–C9 | 180.0002 |
| C7–C2–C3–C6 | 0 | N3–C2–C3–C8 | 2.4607 | C2–C1–C6–C5 | 0.0423 | H1–C1–C6–C5 | 179.9989 |
| H2–C4–C5–N1 | 180.0017 | C1–C2–N3–H5 | 169.5011 | C1–C2–C3–C4 | 0.0003 | C1–C2–C3–C4 | 0.0018 |
| H3–C5–N1–C1 | 180.0021 | C2–C3–C4–C7 | 179.9751 | C8–C2–C3–C4 | 179.9084 | C1–C2–C3–C7 | 180.0008 |

### 3.2. Electronic structures and charges

Natural bond orbital (NBO) analysis was performed in order to analyze the charge populations of the dyes 3,4-pyridinedicarbonitrile, 3-aminophthalonitrile, 4-aminophthalonitrile and 4-methylphthalonitrile. Charge distributions in C, N and H atoms were observed

because of the different electronegativity, the electrons transferred from C atoms to C, N atoms, C atoms to H, N atoms to H atom. The natural charges of different groups are the sum of every atomic natural charge in the group. These data indicate that the cyanine and amide groups are acceptors, while the acetic groups are donors, and the charges were transferred through chemical bonds.

The frontier molecular orbitals (MO) energies of the dyes 3,4-pyridinedicarbonitrile, 3-nitrophthalonitrile, 4-aminophthalonitrile and 4-methylphthalonitrile are shown in Fig. 2. The HOMO–LUMO gap of the dye 3,4--pyridinedicarbonitrile, 3-aminophthalonitrile, 4-aminophthalonitrile and 4-methylphthalonitrile in vacuum is 5.96 eV, 5.54 eV, 5.57 eV, and 5.76 eV, respectively.

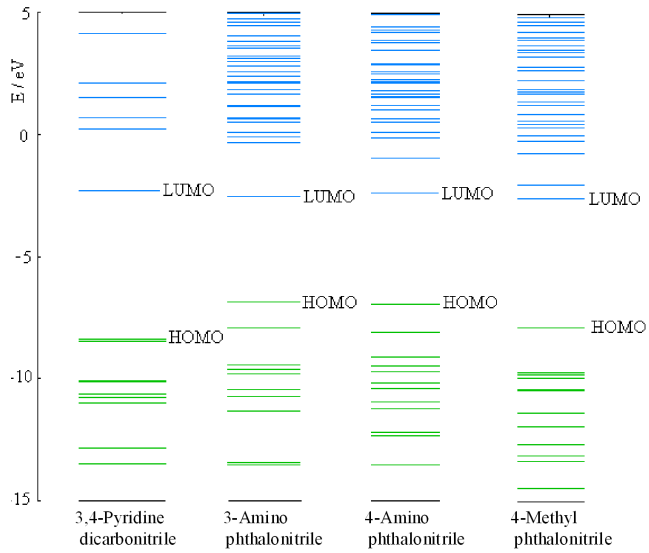


Fig. 2. The frontier molecular orbital energies of the dyes 3,4-pyridinedicarbonitrile, 3-aminophthalonitrile, 4-aminophthalonitrile, and 4-methylphthalonitrile.

While the calculated HOMO and LUMO energies of the bare $Ti_{38}O_{76}$ cluster as a model for nanocrystalline are −6.55 and −2.77 eV, respectively, resulting in a HOMO–LUMO gap of 3.78 eV, the lowest transition is reduced to 3.20 eV according to TD-DFT, and this value is slightly smaller than typical band gap of $TiO_2$ nanoparticles with nm size [35]. Furthermore, the HOMO, LUMO and HOMO–LUMO gap of $(TiO_2)_{60}$ cluster is −7.52, −2.97, and 4.55 eV (B3LYP/VDZ), respectively [36]. Taking into account of the cluster size effects and the calculated HOMO, LUMO, HOMO–LUMO gap of the dyes 3,4-pyridinedicarbonitrile, 3-aminophthalonitrile, 4-aminophthalonitrile and 4-methylphthalonitrile, $Ti_{38}O_{76}$ and $(TiO_2)_{60}$ clusters, we can find that the HOMO energies of these dyes fall within the $TiO_2$ gap.

The above data also reveal the interfacial electron transfer between semiconductor $TiO_2$ electrode and the dye sensitizers 3,4-pyridinedicarbonitrile, 3-aminophthalonitrile, 4-aminophthalonitrile and 4-methylphthalonitrile are electron injection processes from excited dyes to the semiconductor conduction band. This is a kind of typical interfacial electron transfer reaction [37].

### *3.3. IR and Raman frequencies*

Figures 3–6 show the IR and Raman spectra of 3,4--pyridinedicarbonitrile, 3-aminophthalonitrile, 4-aminophthalonitrile and 4-methylphthalonitrile. The strongest IR absorption for 3,4-pyridinedicarbonitrile corresponds to the vibrational mode 28 near about 1614 $cm^{-1}$, which corresponds to stretching mode of C=C bonds. The next stronger IR absorption is attributed to vibrational mode 16 near about 867 $cm^{-1}$, corresponding to the torsion mode of C–H bonds. In the Raman spectra, however, the strongest activity mode is the vibrational mode 29 near about 2345 $cm^{-1}$, which corresponds to stretching mode of C≡N. The strongest IR absorption for 3-aminophthalonitrile corresponds to the vibrational mode 6 near about 290 $cm^{-1}$, which is the out of plane bending mode of C≡N. The next stronger IR absorption is attributed to vibrational mode 35 near about 1664 $cm^{-1}$, corresponds to stretching mode of C=C bonds. In the Raman spectra, however, the strongest activity mode is the vibrational mode 37 near about 2338 $cm^{-1}$, which corresponds to stretching mode of C≡N. The strongest IR absorption for 4-aminophthalonitrile corresponds to the vibrational mode 8 near about 387 $cm^{-1}$, which is the wagging mode of C–H bonds. The next stronger IR absorption is attributed to vibrational mode 35 near about 1666 $cm^{-1}$, corresponds to stretching mode of C=C bonds. In the Raman spectra, however, the strongest activity mode is the vibrational mode 36 near about 2329 $cm^{-1}$, which corresponds to stretching mode of C≡N. The strongest IR absorption for 4-methylphthalonitrile corresponds to the vibrational mode 19 near about 846 $cm^{-1}$, which is the ring breathing mode of C–C bonds. The next stronger IR absorption is attributed to vibrational mode 37 near about 1639 $cm^{-1}$, corresponds to stretching mode of C=C bonds. In the Raman spectra, however, the strongest activity mode is the vibrational mode 38 near about 2337 $cm^{-1}$, which corresponds to stretching mode of C≡N.

### *3.4. Polarizability and hyperpolarizability*

Polarizabilities and hyperpolarizabilities characterize the response of a system in an applied electric field [38]. They determine not only the strength of molecular interactions (long-range intermolecular induction, dispersion forces, etc.) as well as the cross-sections of different scattering and collision processes, but also the nonlinear optical properties (NLO) of the system [39, 40]. It has been found that the dye sensitizer hemicyanine system, which has high NLO property, usually possesses high photoelectric conversion performance [41]. In order to investigate the relationships among photocurrent generation, molecular structures and NLO, the polarizabilities and hyperpolarizabilities of 3,4-pyridinedicarbonitrile, 3-aminophthalonitrile, 4-aminophthalonitrile and

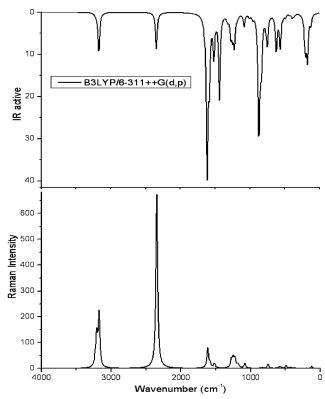


Fig. 3. The calculated IR activity and Raman activity vs. vibration frequency of 3,4-pyridinedicarbonitrile.

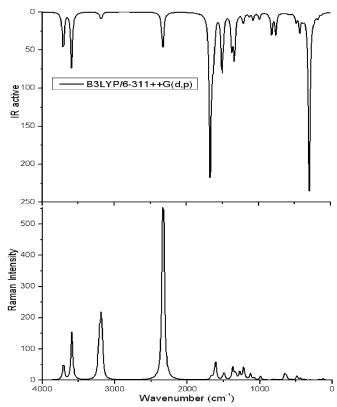


Fig. 4. As in Fig. 3, but for 3-aminophthalonitrile.

4-methylphthalonitrile were calculated. Here, the polarizability and the first hyperpolarizabilities are computed using B3LYP/6-311++G(d,p) method. The definition [39, 40] for the isotropic polarizability is:

$$\alpha = \tfrac{1}{3}\left(\alpha_{XX} + \alpha_{YY} + \alpha_{ZZ}\right).$$

The polarizability anisotropy invariant is

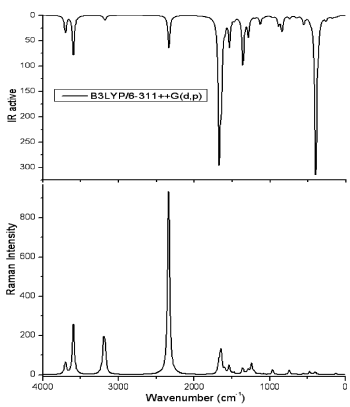


Fig. 5. As in Fig. 3, but for 4-aminophtholonitrile.

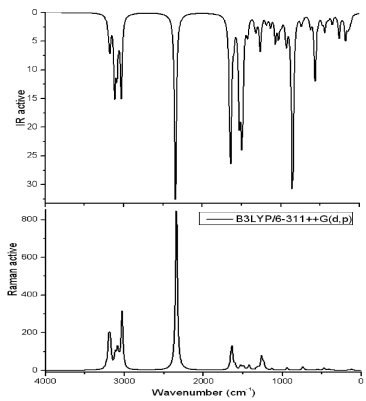


Fig. 6. As in Fig. 3, but for 4-methylphthalanitrile.

$$\Delta\alpha = \left\{\tfrac{1}{2}\left[\left(\alpha_{XX} - \alpha_{YY}\right)^2 + \left(\alpha_{YY} - \alpha_{ZZ}\right)^2 + \left(\alpha_{ZZ} - \alpha_{XX}\right)^2\right]\right\}^{\frac{1}{2}}$$

and the average hyperpolarizability is

$$\beta_{\|} = \tfrac{1}{5}\sum_i \left(\beta_{iiZ} + \beta_{iZi} + \beta_{Zii}\right),$$

where $\alpha_{XX}$, $\alpha_{YY}$ and $\alpha_{ZZ}$ are tensor components of polarizability; $\beta_{iiZ}$, $\beta_{iZi}$, and $\beta_{Zii}$ ($i$ from $X$ to $Z$) are tensor components of hyperpolarizability.

Tables II and III list the values of the polarizabilities and hyperpolarizabilities of the dyes 3,4-pyridinedicarbonitrile, 3-aminophthalonitrile, 4-aminophthalonitrile and 4-methylphthalonitrile. In addition to the individual tensor components of the polarizabilities and the first hyperpolarizabilities, the isotropic polarizability, polarizability anisotropy invariant and hyperpolarizability are also calculated. The calculated isotropic polarizability of 3,4-pyridinedicarbonitrile, 3-aminophthalonitrile, 4--aminophthalonitrile and 4-methylphthalonitrile is 94.76, 112.71, 115.49 and 115.10 atomic units (a.u.), respectively. However, the calculated isotropic polarizability of JK16, JK17, dye 1, dye 2, D5, DST and DSS is 759.9, 1015.5, 694.7, 785.7, 510.6, 611.2 and 802.9 a.u., respectively [42, 43]. The above data indicate that the donor-conjugate $\pi$ bridge–acceptor (D-$\pi$-A) chain-like dyes have stronger response for external electric field. Whereas, for dye sensitizers D5, DST, DSS, JK16, JK17, dye 1 and dye 2, on the basis of the published photo--to-current conversion efficiencies, the similarity and the difference of geometries, and the calculated isotropic polarizabilities, it is found that the longer the length of the conjugate bridge in similar dyes, the larger the polarizability of the dye molecule, and the lower the photo-to--current conversion efficiency. This may be due to the fact that the longer conjugate $\pi$ bridge enlarged the delocalization of electrons, thus it enhanced the response of the external field, but the enlarged delocalization may be not favorable to generate charge separated state effectively. So it induces the lower photo-to-current conversion efficiency.

TABLE II

Polarizability ($\alpha$) of the dyes 3,4-pyridinedicarbonitrile, 3-aminophthalonitrile, 4-aminophthalonitrile and 4-methylphthalonitrile (in a.u.).

| Dyes | $\alpha_{xx}$ | $\alpha_{xy}$ | $\alpha_{yy}$ | $\alpha_{xz}$ | $\alpha_{yz}$ | $\alpha_{zz}$ | $\alpha$ | $\Delta\alpha$ |
|---|---|---|---|---|---|---|---|---|
| 3,4-pyridinedicarbonitrile | 129.215 | −2.938 | 107.116 | 0.000059 | −0.00014 | 47.965 | 94.76 | 72.76 |
| 3-aminophthalonitrile | 144.22 | 5.113 | 136.74 | 0.1023 | −0.2269 | 57.19 | 112.71 | 83.54 |
| 4-aminophthalonitrile | 169.10 | 1.50 | 120.18 | −0.33 | −0.12 | 57.19 | 115.49 | 97.17 |
| 4-methylphthalonitrile | 162.04 | 2.072 | 122.60 | −0.00013 | −0.00018 | 60.68 | 115.10 | 88.49 |

TABLE III

Hyperpolarizability ($\beta$) of the dyes 3,4-pyridinedicarbonitrile, 3-aminophthalonitrile, 4-aminophthalonitrile, and 4-methylphthalonitrile (in a.u.).

| Dyes | $\beta_{xxx}$ | $\beta_{xxy}$ | $\beta_{xyy}$ | $\beta_{yyy}$ | $\beta_{xxz}$ | $\beta_{xyz}$ | $\beta_{yyz}$ | $\beta_{xzz}$ | $\beta_{yzz}$ | $\beta_{zzz}$ | $\beta_{ii}$ |
|---|---|---|---|---|---|---|---|---|---|---|---|
| 3,4-pyridinedicarbonitrile | −8.221 | −52.465 | −43.089 | 77.523 | −0.0008 | −0.0001 | −0.0001 | −38.806 | 12.305 | 0.0002 | 0.0042 |
| 3-aminophthalonitrile | 103.03 | −43.33 | 17.187 | −127.09 | 5.527 | −0.6355 | 4.663 | −52.414 | −47.17 | 5.167 | 9.214 |
| 4-aminophthalonitrile | −0.0663 | −265.78 | −14.77 | 96.71 | 12.58 | 2.968 | 3.623 | 64.93 | −15.89 | 7.56 | 14.257 |
| 4-methylphthalonitrile | 175.92 | −75.168 | −0.716 | 10.05 | 0.0037 | −0.0001 | −0.0013 | −48.98 | −11.33 | 0.0032 | 0.00336 |

### *3.5. Electronic absorption spectra and sensitized mechanism*

Electronic absorption spectra of 3,4-pyridinedicarbonitrile, 3-aminophthalonitrile, 4-aminophthalonitrile and 4-methylphthalonitrile in vacuum and solvent were performed using TD-DFT(PBE1PBE)/6-311++G(d,p) calculations, and the results are shown in Figs. 7–10. It is observed that the absorption in the visible region is much weaker than that in the UV region for 3,4--pyridinedicarbonitrile, 3-aminophthalonitrile, 4-aminophthalonitrile and 4-methylphthalonitrile. The results of TD-DFT have an appreciable redshift in vacuum and solvent. The discrepancy between vacuum and solvent effects in TD-DFT calculations may result from two aspects. The first aspect is smaller gap of materials which induces smaller excited energies. The other is solvent effects. Experimental measurements of electronic absorptions are usually performed in solution. Solvent, especially polar solvent, could affect the geometry and electronic structure as well as the properties of molecules through the long-range interaction between solute molecule and solvent molecule. For these reasons, the TD-DFT calculation is more difficult to make consistent with quantitatively, so TD-DFT calculation with polar solvent measurable. Though the discrepancy exists, the TD-DFT calculations are capable of describing the spectral features of 3,4-pyridinedicarbonitrile, 3-aminophthalonitrile, 4-aminophthalonitrile and 4-methylphthalonitrile, because of the agreement of line shape and relative strength as compared with the vacuum and solvent.

The HOMO–LUMO gap of 3,4-pyridinedicarbonitrile, 3-aminophthalonitrile, 4-aminophthalonitrile and 4-methylphthalonitrile in acetonitrile at PBE1PBE/6-311++G(d,p) theory level is smaller than that in vacuum. This fact indicates that the solvent effects stabilize the frontier orbitals of 3,4-pyridinedicarbonitrile, 3-aminophthalonitrile, 4-aminophthalonitrile and 4-methylphthalonitrile, so it induces the smaller intensities and redshift of the absorption as compared with that in vacuum.

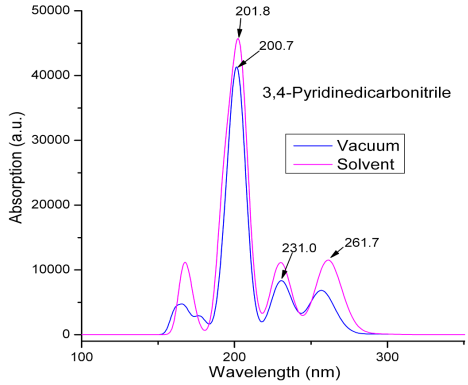


Fig. 7. Calculated electronic absorption spectra of 3,4--pyridinedicarbonitrile.

In order to obtain the microscopic information about the electronic transitions, the corresponding MO properties are checked. The absorption in visible and near-UV region is the most important region for photo-to-current conversion, so only the 20 lowest singlet/singlet transitions of the absorption band in visible and near-UV region for 3,4-pyridinedicarbonitrile, 3-aminophthalonitrile, 4-aminophthalonitrile and 4-methylphthalonitrile are listed in Tables IV–VII. The data of Tables IV–VII and Fig. 11 are based on the 6-311++G(d,p) results with solvent effects involved.

This indicates that the transitions are photoinduced charge transfer processes, thus the excitations generate charge separated states, which should favour the electron injection from the excited dyes to semiconductor surface.

The solar energy to electricity conversion efficiency ($\eta$) under AM 1.5 white-light irradiation can be obtained

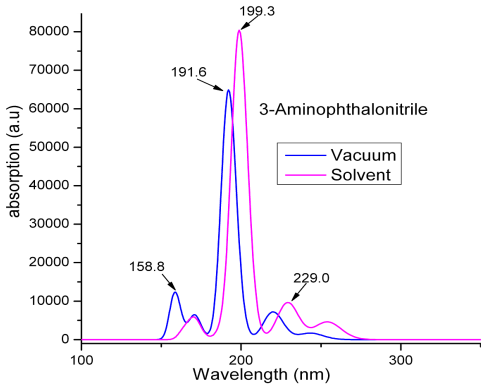


Fig. 8. As in Fig. 7, but for 3-aminophthalonitrile.

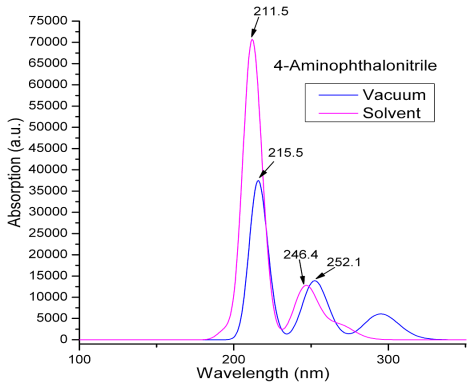


Fig. 9. As in Fig. 7, but for 4-aminophthalonitrile.

from the following formula:

$$\eta(\%) = \frac{J_{\rm sc}[\text{mA cm}^{-2}]V_{\rm oc}[\text{V}]\text{ff}}{I_0[\text{mW cm}^{-2}]} \times 100,$$

where $I_0$ is the photon flux, $J_{\rm sc}$ is the short-circuit photocurrent density, and $V_{\rm oc}$ is the open-circuit photovoltage, and ff represents the fill factor [44]. At present, the $J_{\rm sc}$, the $V_{\rm oc}$, and the ff are only obtained by experiment, the relationship among these quantities and the

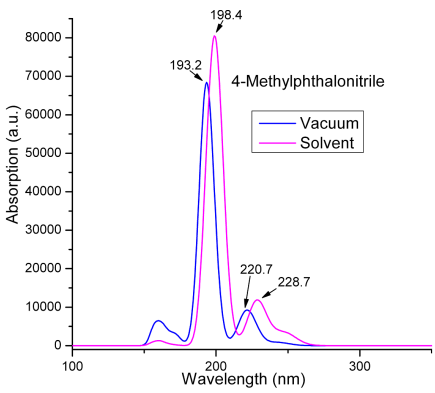


Fig. 10. As in Fig. 7, but for 4-methylphthalonitrile.

electronic structure of dye is still unknown. The analytical relationship between $V_{\rm oc}$ and $E_{\rm LUMO}$ may exist. According to the sensitized mechanism (electron injected from the excited dyes to the semiconductor conduction band) and single electron and single state approximation, there is an energy relationship

$$eV_{\rm oc} = E_{\rm LUMO} - E_{\rm CB},$$

where $E_{\rm CB}$ is the energy of the semiconductor's conduction band edge. So the $V_{\rm oc}$ may be obtained applying the following formula:

$$V_{\rm oc} = (E_{\rm LUMO} - E_{\rm CB})/e\,.$$

It induces that the higher the $E_{\rm LUMO}$, the larger the $V_{\rm oc}$.

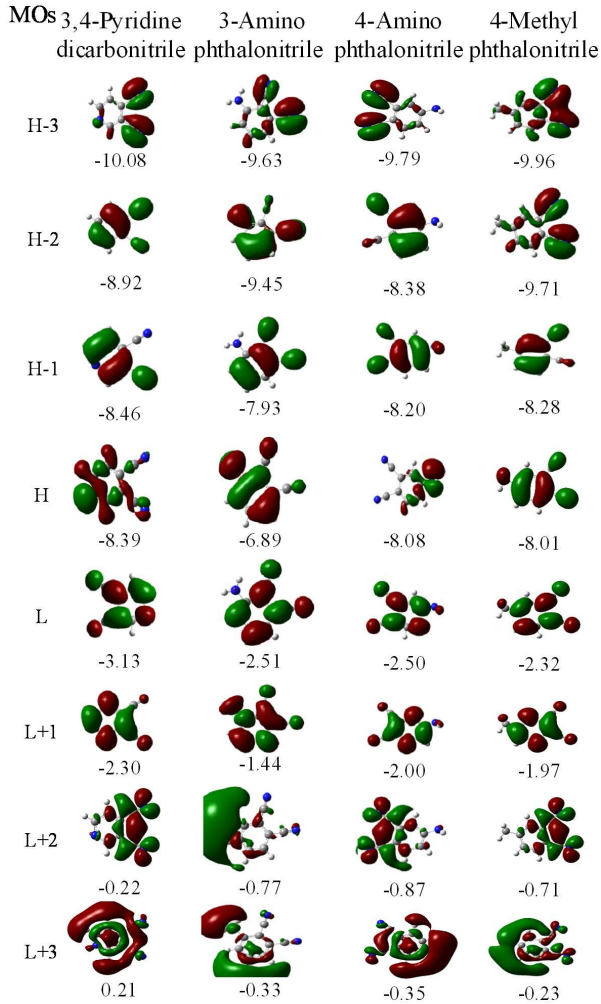


Fig. 11. Isodensity plots (isodensity contour = 0.02 a.u.) of the frontier orbitals of the dyes and corresponding orbital energies (in eV).

The results of organic dye sensitizer JK16 and JK17 [42], D-ST and D-SS also proved the tendency [45] (JK16: $E_{\rm LUMO} = -2.73$ eV, $V_{\rm oc} = 0.74$ V; JK17: $E_{\rm LUMO} = -2.87$ eV, $V_{\rm oc} = 0.67$ V; D-SS: $E_{\rm LUMO} = -2.91$ eV, $V_{\rm oc} = 0.70$ V; D-ST: $E_{\rm LUMO} = -2.83$ eV, $V_{\rm oc} = 0.73$ V).

TABLE IV

Computed excitation energies, electronic transition configurations and oscillator strengths ($f$) for the optical transitions with $f > 0.01$ of the absorption bands in visible and near-UV region for the dye 3,4-pyridinedicarbonitrile in acetonitrile.

| State | Configurations composition (corresponding transition orbitals) | Excitation energy [eV/nm] | Oscillator strength ($f$) |
|---|---|---|---|
| 2 | −0.13 (31 → 34) −0.24 (31 → 35)<br>0.61 (33 → 34) −0.13 (33 → 35) | 4.79/258.55 | 0.14 |
| 4 | 0.57 (31 → 34) 0.17 (33 → 34)<br>0.27 (33 → 35) | 5.44/227.70 | 0.14 |
| 6 | 0.12 (27 → 34) −0.26 (31 → 34)<br>0.54 (33 → 35) | 6.17/200.75 | 0.52 |
| 8 | −0.13 (28 → 34) 0.60 (31 → 35)<br>0.12 (33 → 34) −0.12 (33 → 35) | 6.47/191.57 | 0.29 |
| 11 | −0.11 (27 → 34) 0.63 (28 → 34)<br>0.10 (29 → 37) 0.12 (31 → 35)<br>−0.12 (32 → 36) | 7.24/171.25 | 0.03 |
| 15 | 0.49 (27 → 34) 0.11 (30 → 36)<br>−0.44 (32 → 36) | 7.41/167.31 | 0.03 |
| 18 | 0.37 (27 → 34) 0.16 (28 → 34)<br>0.51 (32 → 36) | 7.59/163.34 | 0.06 |
| 20 | 0.10 (27 → 35) 0.67 (32 → 37) | 7.97/155.44 | 0.08 |

TABLE V

Computed excitation energies, electronic transition configurations and oscillator strengths ($f$) for the optical transitions with $f > 0.01$ of the absorption bands in visible and near-UV region for the dye 3-aminophthalonitrile in solvent.

| State | Configurations composition (corresponding transition orbitals) | Excitation energy [eV/nm] | Oscillator strength ($f$) |
|---|---|---|---|
| 3 | 0.35749 (35 → 39) 0.59993 (36 → 38) | 4.8856/253.77 | 0.0635 |
| 4 | 0.60145 (35 → 38) −0.26698 (36 → 39) | 5.4165/228.90 | 0.1330 |
| 5 | 0.13865 (33 → 38) 0.21405 (35 → 38)<br>0.13087 (35 → 39) 0.55944 (36 → 39) | 6.2145/199.51 | 0.3921 |
| 6 | 0.54145 (35 → 39) −0.25188 (36 → 38)<br>−0.14768 (36 → 39) | 6.2609/198.03 | 0.7261 |
| 8 | 0.67969 (37 → 40) −0.16019 (37 → 41) | 6.6025/187.78 | 0.0274 |
| 12 | 0.64383 (33 → 38) −0.14077 (34 → 40) | 7.1527/173.34 | 0.0181 |
| 13 | 0.15701 (37 → 40) 0.64019 (37 → 41)<br>0.17806 (37 → 45) | 7.2886/170.11 | 0.0588 |
| 18 | −0.17371 (37 → 41) 0.60718 (37 → 42)<br>0.27148 (37 → 45) | 7.5653/163.89 | 0.0308 |

Certainly, this formula expects further test by experiment and theoretical calculation. The $J_{sc}$ is determined by two processes, one is the rate of electron injection from the excited dyes to the conduction band of semiconductor, and the other is the rate of redox between the excited dyes and electrolyte. Electrolyte affect on the redox processes is very complex, and it is not taken into account in the present calculations. On the basis of the analysis of excitation energies, electronic transition configurations, oscillator strengths and molecular orbitals of 3,4-pyridinedicarbonitrile, 3-aminophthalonitrile, 4--aminophthalonitrile and 4-methylphthalonitrile in UV--Vis region, we find that most oscillator strengths for the excited states with intramolecular electron transfer character of 4-aminophthalonitrile are larger than that of 3,4-pyridinedicarbonitrile, 3-aminophthalonitrile and 4-methylphthalonitrile.

This indicates that most of excited states of 4-aminophthalonitrile have larger absorption coefficient, and then with shorter lifetime for the excited states, so it results in

TABLE VI

Computed excitation energies, electronic transition configurations and oscillator strengths ($f$) for the optical transitions with $f > 0.01$ of the absorption bands in visible and near-UV region for the dye 4-aminophthalonitrile in solvent.

| State | Configurations composition (corresponding transition orbital) | Excitation energy [eV/nm] | Oscillator strength ($f$) |
|---|---|---|---|
| 1 | −0.13772 (36 → 39) 0.62208 (37 → 38) −0.18956 (37 → 39) | 4.0351/307.27 | 0.1579 |
| 2 | 0.31856 (36 → 38) 0.16886 (37 → 38) 0.56654 (37 → 39) | 4.8193/257.27 | 0.2310 |
| 3 | 0.54733 (36 → 38) 0.14821 (36 → 39) −0.26869 (37 → 39) | 5.6045/221.22 | 0.6325 |
| 5 | 0.57246 (35 → 38) −0.12001 (36 → 38) 0.31288 (36 → 39) | 6.2357/198.83 | 0.1277 |
| 7 | −0.34228 (35 → 38) 0.53442 (36 → 39) | 6.4820/191.28 | 0.2886 |
| 11 | 0.12583 (34 → 40) 0.10658 (34 → 41) 0.62630 (35 → 39) 0.14546 (37 → 42) | 7.2485/171.05 | 0.0606 |
| 13 | 0.40772 (32 → 38) 0.53526 (37 → 42) | 7.5963/163.22 | 0.1083 |
| 16 | 0.22620 (30 → 38) 0.40714 (32 → 38) 0.13547 (33 → 40) 0.14380 (35 → 39) −0.32147 (37 → 42) −0.27250 (37 → 43) 0.13633 (37 → 44) | 7.7219/160.56 | 0.0354 |
| 20 | 0.47147 (28 → 38) 0.45804 (29 → 38) | 7.9748/155.47 | 0.0149 |

TABLE VII

Computed excitation energies, electronic transition configurations and oscillator strengths ($f$) for the optical transitions with $f > 0.01$ of the absorption bands in visible and near-UV region for the dye 4-methylphthalonitrile in solvent.

| State | Configurations composition (corresponding transition orbitals) | Excitation energy [eV/nm] | Oscillator strength ($f$) |
|---|---|---|---|
| 1 | −0.37690 (36 → 38) −0.25951 (36 → 39) 0.44013 (37 → 38) −0.31582 (37 → 39) | 5.0105/247.45 | 0.0449 |
| 2 | 0.40666 (36 → 38) −0.12746 (36 → 39) 0.43828 (37 → 38) 0.27222 (37 → 39) | 5.4316/228.27 | 0.1628 |
| 3 | −0.35497 (36 → 38) 0.49676 (37 → 39) | 6.1917/200.24 | 0.8644 |
| 4 | 0.58161 (36 → 39) 0.20114 (37 → 38) −0.11722 (37 → 39) | 6.3807/194.31 | 0.4258 |
| 15 | 0.62695 (30 → 38) 0.12594 (32 → 40) −0.13672 (33 → 40) −0.16394 (34 → 39) 0.13359 (35 → 41) | 7.6942/161.14 | 0.0102 |

the higher electron injection rate of the 4-aminophthalonitrile, then it leads to the larger $J_{sc}$ of 4-aminophthalonitrile. On the basis of above analysis, the 4-aminophthalonitrile has better performance in DSSC than that of 3,4-pyridinedicarbonitrile, 3-aminophthalonitrile and 4-methylphthalonitrile.

## 4. Conclusions

The geometries, electronic structures, polarizabilities, and hyperpolarizabilities of dyes 3,4-pyridinedicarbonitrile, 3-aminophthalonitrile, 4-aminophthalonitrile and 4-methylphthalonitrile were studied by using density functional theory with hybrid functional B3LYP, and the UV-Vis spectra were investigated by using TD-DFT methods. The NBO results suggest that 3,4-pyridinedicarbonitrile, 3-aminophthalonitrile, 4--aminophthalonitrile, and 4-methylphthalonitrile are all ($D$–$\pi$–$A$) systems. The calculated isotropic polarizability of 3,4-pyridinedicarbonitrile, 3-aminophthalonitrile, 4-aminophthalonitrile, and 4-methylphthalonitrile is 94.76, 112.71, 115.49 and 115.10 a.u., respectively. The calculated polarizability anisotropy invariant of 3,4-pyridinedicarbonitrile, 3-aminophthalonitrile, 4-aminophthalonitrile, and 4-methylphthalonitrile is 72.76, 83.54, 97.17 and 88.49 a.u., respectively. The hyperpolarizabilities of 3,4-pyridinedicarbonitrile, 3-aminophthalonitrile, 4-aminophthalonitrile, and 4--methylphthalonitrile is 0.0042, 9.214, 14.257, 0.0033 (in a.u.), respectively. The frequencies of strongest IR absorption for 3,4-pyridinedicarbonitrile, 3-aminophthalonitrile, 4-aminophthalonitrile and 4-methylphthalonitrile

are 1614 $cm^{-1}$, 290 $cm^{-1}$, 387 $cm^{-1}$ and 846 $cm^{-1}$ and the frequencies of strongest Raman activity for 3,4--pyridinedicarbonitrile, 3-aminophthalonitrile, 4-aminophthalonitrile and 4-methylphthalonitrile are 2345 $cm^{-1}$, 2338 $cm^{-1}$, 2329 $cm^{-1}$, 2337 $cm^{-1}$, respectively. The electronic absorption spectral features in visible and near-UV region were assigned based on the qualitative agreement to TD-DFT calculations. The absorptions are all ascribed to $\pi \rightarrow \pi^*$ transition. The three excited states with the lowest excited energies of 3,4-pyridinedicarbonitrile, 3-aminophthalonitrile, 4--aminophthalonitrile and 4-methylphthalonitrile are photoinduced electron transfer processes that contributes sensitization of photo-to-current conversion processes. The interfacial electron transfer between semiconductor $TiO_2$ electrode and dye sensitizer 3,4-pyridinedicarbonitrile, 3-aminophthalonitrile, 4-aminophthalonitrile and 4-methylphthalonitrile is electron injection process from excited dyes as donor to the semiconductor conduction band. Based on the comparative analysis of geometries, electronic structures, and spectrum properties between 3,4-pyridinedicarbonitrile, 3-aminophthalonitrile, 4-aminophthalonitrile, and 4-methylphthalonitrile the role of amide and methyl groups in phthalonitrile is as follows: it enlarged the distance between electron donor group and semiconductor surface, and decreased the timescale of the electron injection rate, resulting in giving lower conversion efficiency. This indicates that the choice of the appropriate conjugate bridge in dye sensitizer is very important to enhance the performance of DSSC.

## Acknowledgments

This work had been partly financially supported by University Grants Commission, Govt. of India, New Delhi, within the Major Research Project scheme under the approval-cum-sanction Nos. F.No.34-5\2008(SR) and 34-1/TN/08.

## References

[1] B. O'Regan, M. Gratzel, *Nature* **353**, 737 (1991).

[2] M. Gratzel, *Nature* **414**, 338 (2001).

[3] N.G. Park, K. Kim, *Phys. Status Solidi A* **205**, 1895 (2008).

[4] Y. Chiba, A. Islam, Y. Watanabe, R. Komiya, N. Koide, L. Han, *Jpn. J. Appl. Phys., Part 2* **45**, L638 (2006).

[5] K. Hara, M. Kurashige, Y. Dan-oh, C. Kasada, A. Shinpo, S. Suga, K. Sayama, H. Arakawa, *New J. Chem.* **27**, 783 (2003).

[6] T. Kitamura, M. Ikeda, K. Shigaki, T. Inoue, N.A. Anderson, X. Ai, T. Lian, S. Yanagida, *Chem. Mater.* **16**, 1806 (2004).

[7] T. Horiuchi, H. Miura, K. Sumioka, S. Uchida, *J. Am. Chem. Soc.* **126,** 12218 (2004).

[8] W.M. Campbell, A.K. Burrell, D.L. Officer, K.W. Jolley, *Coord. Chem. Rev.* **248**, 1363 (2004).

[9] K.R.J. Thomas, J.T. Lin, Y.C. Hsu, K.C. Ho, *Chem. Commun.*, 4098 (2005).

[10] D.P. Hagberg, T. Edvinsson, T. Marinado, G. Boschloo, A. Hagfeldt, L. Sun, *Chem. Commun.* 21, 2245 (2006).

[11] S.L. Li, K.J. Jiang, K.F. Shao, L.M. Yang, *Chem. Commun.* 26, 2792 (2006).

[12] N. Koumura, Z.S. Wang, S. Mori, M. Miyashita, E. Suzuki, K. Hara, *J. Am. Chem. Soc.* **128**, 14256 (2006).

[13] S. Kim, J.W. Lee, S.O. Kang, J. Ko, J.H. Yum, S. Fantacci, F. De Angellis, D. Di Censo, M.K. Nazeeruddin, M. J. Gratzel, *J. Am. Chem. Soc.* **128**, 16701 (2006).

[14] Z.S. Wang, Y. Cui, K. Hara, Y. Danoh, C. Kasada, A. Shinpo, *Adv. Mater.* **19,** 1138 (2007).

[15] T. Edvinsson, C. Li, N. Pschirer, J. Schoneboom, F. Eickemeyer, R. Sens, G. Boschloo, A. Herrmann, K. Mullen, A. Hagfeldt, *J. Phys. Chem. C* **111,** 15137 (2007).

[16] M. Wang, M. Xu, D. Shi, R. Li, F. Gao, G. Zhang, Z. Yi, R. Humphry-Baker, P. Wang, S.M. Zakeeruddin, M. Gratzel, *Adv. Mater.* **20**, 4460 (2008).

[17] D. Shi, N. Pootrakuchote, Z. Yi, M. Xu, S.M. Zakeeruddin, M. Gratzel, P.J. Wang, *Phys. Chem. C* **112,** 17478 (2008).

[18] G. Zhou, N. Pschirer, J.C. Schoneboom, F. Eickemeyer, M. Baumgarten, K. Mullen, *Chem. Mater.* **20**, 1808 (2008).

[19] J.T. Lin, P.C. Chen, Y.S. Yen, Y.C. Hsu, H.H. Chou, M.C.P. Yeh, *Org. Lett.* **11**, 97 (2009).

[20] G. Zhang, Y. Bai, R. Li, D. Shi, S. Wenger, S.M. Zakeeruddin, M. Gratzel, P. Wang, *Energy Environs. Sci.* **2**, 92 (2009).

[21] M. Xu, S. Wenger, H. Bara, D. Shi, R. Li, Y. Zhou, S.M. Zakeeruddin, M. Gratzel, P. Wang, *J. Phys. Chem. C* **113**, 2966 (2009).

[22] X.H. Zhang, C. Li, W.B. Wang, X.X. Cheng, X.S. Wang, B.W. Zhang, *J. Mater. Chem.* **17**, 642 (2007).

[23] M. Liang, W. Xu, F. Cai, P. Chen, B. Peng, J. Chen, Z. Li, *J. Phys. Chem. C* **111**, 4465 (2007).

[24] W. Xu, B. Peng, J. Chen, M. Liang, F. Cai, *J. Phys. Chem. C* **112**, 874 (2008).

[25] S. Ito, H. Miura, S. Uchida, M. Takata, K. Sumioka, P. Liska, P. Comte, P. Pechy, M. Gratzel, *Chem. Commun.* 41, 5194 (2008).

[26] M.J. Frisch, G.W. Trucks, H.B. Schlegel, G.E. Scuseria, M.A. Robb, J.R. Cheeseman, J.A. Montgomery Jr., T. Vreven, K.N. Kudin, J.C. Burant, J.M. Millam, S.S. Iyengar, J. Tomasi, V. Barone, B. Mennucci, M. Cossi, G. Scalmani, N. Rega, G.A. Petersson, H. Nakatsuji, M. Hada, M. Ehara, K. Toyota, R. Fukuda, J. Hasegawa, M. Ishida, T. Nakajima, Y. Honda, O. Kitao, H. Nakai, M. Klene, X. Li, J.E. Knox, H.P. Hratchian, J.B. Cross, C. Adamo, J. Jaramillo, R. Gomperts, R.E. Stratmann, O. Yazyev, A.J. Austin, R. Cammi, C. Pomelli, J.W. Ochterski, P.Y. Ayala, K. Morokuma, G.A. Voth, P. Salvador, J.J. Dannenberg, V.G. Zakrzewski, S. Dapprich, A.D. Daniels, M.C. Strain, O. Farkas, D.K. Malick, A.D. Rabuck, K. Raghavachari, J.B. Foresman, J.V. Ortiz, Q. Cui, A.G. Baboul, S. Clifford, J. Cioslowski, B.B. Stefanov, G. Liu, A. Liashenko, P. Piskorz, I. Komaromi, R.L. Martin, D.J. Fox, T. Keith, M.A. Al-Laham, C.Y. Peng, A. Nanayakkara, M. Challacombe, P.M.W. Gill, B. Johnson, W. Chen, M.W. Wong, C. Gonzalez, J.A. Pople, Gaussian 03, Gaussian, Inc., Pittsburgh, PA, 2003.

[27] A.D. Becke, *J. Chem. Phys.* **98**, 5648 (1993).

[28] B. Miehlich, A. Savin, H. Stoll, H. Preuss, *Chem. Phys. Lett.* **157**, 200 (1989).

[29] C. Lee, W. Yang, R.G. Parr, *Phys. Rev. B.* **37**, 785 (1988).

[30] P.L. Polavarapu, *J. Phys. Chem.* **94**, 8106 (1990).

[31] G. Keresztury, S. Holly, J. Varga, G. Besenyei, A.Y. Wang, J.R. Durig, *Spectrochim. Acta* **49A**, 1993 (2007).

[32] G. Keresztury, in: *Handbook of Vibrational Spectroscopy*, Vol. 1 Eds. J.M. Chalmers, P.R. Griffiths, Wiley, Chichester 2001, p. 71.

[33] V. Barone, M. Cossi, *J. Phys. Chem. A* **102**, 1995 (1998).

[34] M. Cossi, N. Rega, G. Scalmani, V. Barone, *J. Comput. Chem.* **24**, 669 (2003).

[35] M.K. Nazeeruddin, F. De Angelis, S. Fantacci, A. Selloni, G. Viscardi, P. Liska, S. Ito, B. Takeru, M. Gratzel, *J. Am. Chem. Soc.* **127**, 16835 (2005).

[36] M.J. Lundqvist, M. Nilsing, P. Persson, S. Lunell, *Int. J. Quantum Chem.* **106**, 3214 (2006).

[37] D.F. Waston, G.J. Meyer, *Ann. Rev. Phys. Chem.* **56**, 119 (2005).

[38] C.R. Zhang, H.S. Chen, G.H. Wang, *Chem. Res. Chin. U.* **20**, 640 (2004).

[39] Y. Sun, X. Chen, L. Sun, X. Guo, W. Lu, *Chem. Phys. Lett.* **381**, 397 (2003).

[40] O. Christiansen, J. Gauss, J.F. Stanton, *Chem. Phys. Lett.* **305**, 147 (1999).

[41] Z.S. Wang, Y.Y. Huang, C.H. Huang, J. Zheng, H.M. Cheng, S.J. Tian, *Synth. Met.* **14**, 201 (2000).

[42] C.R. Zhang, Y.Z. Wu, Y.H. Chen, H.S. Chen, *Acta Phys. Chim. Sin.* **25**, 53 (2009).

[43] A. Seidl, A. Gorling, P. Vogl, J.A. Majewski, M. Levy, *Phys. Rev. B* **53**, 3764 (1996).

[44] K. Hara, T. Sato, R. Katoh, A. Furube, Y. Ohga, A. Shinpo, S. Suga, K. Sayama, H. Sugihara, H. Arakawa, *J. Phys. Chem. B* **107**, 597 (2003).

[45] C.R. Zhang, Z.J. Liu, Y.H. Chen, H.S. Chen, Y.Z. Wu, L.H. Yuan, *J. Mol. Struct.* **899**, 86 (2009).